

Unfolding the Greener Path: A Global Subnational Analysis of the Environmental Kuznets Curve

Preliminary draft

The latest version of this paper is available at this [link](#).

Angelo dos Santos, Oscar Morales, Jere R. Behrman, Emily Hannum, Fan Wang*

October 6, 2025

Abstract

This paper provides the first global subnational analysis of the Environmental Kuznets Curve (EKC), relating GDP per capita and air pollution by aerosol. We use satellite data for Aerosol Optical Depth (AOD), a proxy for air pollution, and merge it with subnational GDP per capita for 2010 and population estimates. Our polynomial and quantile regressions confirm a robust inverted U-shaped relationship between income and pollution globally. However, we find significant heterogeneity across the air pollution distribution, with lower pollution quantiles exhibiting a flatter curve than higher pollution ones. Estimated Pollution-GDP elasticities confirm the overall EKC trend globally, with poorer regions exhibiting positive elasticities, while richer regions show negative magnitudes. However, considerable variation exists within regions, emphasizing that the development-pollution trajectory is not uniform.

*[Angelo dos Santos](#): Population Studies Center, University of Pennsylvania, PA, USA; [Oscar Morales](#): Graduate Group in Demography and Department of Economics, University of Pennsylvania, Philadelphia, PA 19104, USA; [Jere R. Behrman](#): Departments of Economics and Sociology and Population Studies Center, University of Pennsylvania, Philadelphia, PA 19104, USA; [Emily Hannum](#): Department of Sociology and Population Studies Center, University of Pennsylvania, PA, USA; [Fan Wang](#): Department of Economics, University of Houston, Houston, Texas, USA. This paper is part of the project "Climate Risk, Pollution, and Childhood Inequalities in Low- and Middle-income Countries," which is supported by National Science Foundation Grant 2230615 (PI: Hannum)

1 Introduction

The Environmental Kuznets Curve (EKC) indicates an inverted U-shaped relationship between economic development and environmental degradation. Initially, as income rises, environmental degradation increases, but decreases when a certain income level is reached, the turning point. After reaching this income level, increases would lead to reductions in environmental degradation. This dynamic is theoretically driven by the elasticity of substitution between consumption and environmental quality (Shibayama and Fraser 2014). Due to its theoretical importance and policy implications, the EKC has been a central topic across various disciplines, including economics ([Grossman and Krueger 1991](#); [Jayachandran 2022](#)), energy studies ([Cohen et al. 2019](#); [Mohsin et al. 2022](#)), and environmental sciences ([Roy Chowdhury and Moran 2012](#); [Stern and Dijk 2017](#)).

Despite the extensive empirical estimation of the EKC across global, regional, and national scales, these studies suffer from data limitations that limit these papers' results. Specifically, the majority of these analyses did not incorporate proper population weights to account for the actual exposure of people to air pollution. Moreover, the use of national-level data does not allow authors to explore within-country heterogeneity, which may hide important variations in the development-environment relationship at a more granular, subnational level. Finally, papers have focused on non-aerosol air pollution — O₃, and CO₂ — indicating a lack of EKC papers that investigate the relationship between income and air pollution by aerosol – PM and AOD ([Stern and Dijk 2017](#)). This specific dimension of air pollution is important to investigate, as this is related to health consequences for populations.

The contributions of this paper are threefold. First, it is the first to document the existence of an EKC globally using subnational income information. Second, we add to the literature on EKC by relating income and air pollution by aerosol as a measure of environmental degradation. Even though there is a large set of papers studying the relationship between development and environmental degradation under an EKC framework, few papers investigate the dynamics of air pollution as income grows. We use AOD as a measure of aerosol pollution, as this is a predictor of PM2.5 and other hazardous factors for environmental degradation, such as smoke and light reduction ([Hao et al. 2024](#); [Hu 2009](#); [Tanasa et al. 2025](#)). Third, this is the first work to estimate the heterogeneous correlations that exist between environmental degradation and economic development across the global location categories. We do this by providing a quan-

tile regression approach and using its results to estimate air pollution by aerosol elasticities for each subnational unit in our dataset.

To estimate our global EKC, we use satellite information, which provides granular information on Aerosol Optical Depth around the globe and population estimates. We merge our population-weighted air pollution exposure measure with subnational GDP per capita to investigate the relationship between economic development and environmental degradation. We use two methodological approaches to verify the existence of the global correlation. First, following the long literature on EKC estimations, we fit polynomials from 1 to 4 degrees to our dataset, allowing us to estimate turning points and curvature of the EKC. Second, to explore possible heterogeneities across the distribution of subnational unit air pollution exposure, we use quantile regressions to correlate economic development and environmental measures for different parts of the distribution. This allows us to use estimated parameters to recover elasticities for each subnational unit and average subregional measures across the globe.

Our results confirm the existence of a U-inverted relationship between GDP per capita and Air pollution by aerosol, which is consistent across polynomial non-linear fits and regional, subregional, country, and subnational samples. Our quantile regressions suggest heterogeneity in this relationship, with lower parts of the air pollution distributions presenting a flatter curve, which is steeper for higher distribution portions. The estimated elasticities follow a theoretical expected pattern around the world, with poorer regions showing average negative elasticities that turn less negative and eventually positive for richer regions. However, there is considerable variation within regions, i.e., average regions with negative elasticities containing subnational units with positive elasticities and vice versa.

2 Data

2.1 Air pollution by aerosols as measured by AOD

Aerosols are ensembles of suspended particles present in the Earth's atmosphere. Atmospheric pollution by aerosols is important to human health and well-being because higher amounts of aerosol particles degrade visibility and can also damage health, especially when there is a higher concentration of PM_{2.5} particles that are smaller than 2.5 micrometers (Jacobsen and Hanley 2009). Aerosol Optical Depth (AOD) is a satellite-based measure that captures the composition, size and concentration of aerosols by measuring the magnitude of atmospheric light

reflection and absorption across the globe (Lenoble, Remer, and Tanre 2013). Scaled between 0 to 1, an AOD value that is less than 0.1 indicates crystal clear sky and clear satellite to earth surface visibility. In contrast, an AOD value close to 1 indicates very hazy conditions (NASA Earth Observatory 2024).

We use AOD measurements based on images collected by the TERRA satellite with its MODIS instruments (Xiong et al. 2020), and we access the data via the NASA EarthData data collection, using the OpenDAP protocol (Cornillon, Gallagher, and Sgouros 2003). On each day in a particular year, tracking along TERRA’s orbital path across the globe, we download AOD data at a spatial resolution of $3\text{km} \times 3\text{km}$ and at all available 5 minute temporal resolution units. For each day, this process generates a vector of latitude-, longitude-, and time-specific AOD measurements.

Within each $1^\circ \times 1^\circ$ longitude–latitude grid (cell), we compute average daily AOD values based on the subset of the daily AOD measurement vector that fall within the geographical boundaries of each cell on that day. Repeating this across days during a year, we generate for each cell, a vector of average daily AOD measurements. During each year, the length of these cell-specific daily average AOD vectors is equal to the number of days in which valid AOD measurements are available for a particular cell. On some days, there might be no cell-specific AOD measurements due to high cloud fraction and invalid reflectance assumptions (Wang et al. 2021) or due to limited overlaps between the cells and the daily orbital path (Xiong et al. 2020).

Using the cell-specific vectors of average daily AOD measurements from a year, we compute annual average AOD exposures for each cell, first averaging over the days in which cell-specific measurements are available, and then separately averaging over all days after complementing the observed averages with interpolated and extrapolated estimates on days without cell-specific measurements. Due to the concentration of missing AOD data in regions with the least population, our population-weighted AOD distributional results based on the raw data and interpolated and extrapolated data are very similar. Our global inequality results presented in the text are based on annual averages of the raw data.¹

1. See Appendix Figure E.1 for a visualization of the number of days in 2010 with AOD measurements across global cells.

2.2 Global gridded population data

In conjunction with the cell-specific AOD data, we generate cell-specific global population estimates based on the Gridded Population of the World Version 4 (GPWv4) dataset from the Center for International Earth Science Information Network ([CIESIN Columbia University 2018](#)). The GPWv4 data contains population statistics from 241 global economies. Data is sourced in most cases from national and local statistical agencies, and when that is not available, sourced from the United Nations.

The gridded GPWv4 data provides total population estimates at 30 arc-second grids ($\sim 1\text{km}$ at the equator), and is globally disaggregated from official population data at the smallest administrative level available. As an illustration, the dataset contains disaggregated population data from 316,461 Brazilian sectors, 43,878 Chinese townships, 5,967 Indian sub-districts, 774 Nigerian local government areas, and 10,535,212 US census blocks. To allow for the calculation population-weighted AOD data, we aggregate the GPWv4 population estimates up to $1^\circ \times 1^\circ$ longitude–latitude grid, which matches up with the resolution of our cell-specific annual average AOD exposures data.

Due to variabilities in census survey and population register data availability, GPWv4 population data are sourced between the years 2001 and 2015, with the center of the calendar year distribution at around 2010. Specifically, data from 27% of the economies are based on 2010 census and population register data, 62% and 83% of the economies' data come from within one and three years of 2010, and about 8% of the economies have data sourced from outside of four years of 2010. To appropriately match up the time-frame of the population and AOD data, we use cell-specific annual average AOD exposure data in 2010.

2.3 Subnational GDP data

We complement global measurements of air pollution by aerosols and population with data on the relative levels of economic development as captured by GDP per capita. Specifically, we use national and subnational from the Gridded global datasets for Gross Domestic Product ([Kummu, Taka, and Guillaume 2018](#)), which is based on subnational GDP per capita data from Gennaioli et al. ([2013](#)). The GDP per capita values are adjusted for purchasing price parity and based on 2005 international dollars.

Gennaioli et al. ([2013](#)) collected subnational GDP data from 1569 subnational first-level or

equivalent administrative units from the largest 110 economies up to 2010. These economies accounted for 97% of global GDP in 2010. Kummu, Taka, and Guillaume (2018) augmented the dataset with national GDP data from economies without subnational data, filling in missing subnational GDP values by interpolating based on geographically and temporally neighboring data-points around missing values, and extended the dataset time-frame to 2015 by extrapolating based on trends up to 2010.

Considering jointly the temporal availability of AOD, pollution, and GDP data, we use the 2010 subnational and national GDP per capita estimates from Kummu, Taka, and Guillaume (2018).

3 Empirical Strategy

3.1 Polynomial fit

To investigate the relationship between economic development and air pollution, we employ an Environmental Kuznets Curve (EKC) framework. The EKC hypothesis states that environmental degradation initially worsens as a country's income per capita increases, but eventually reaches a turning point after which environmental quality improves with further economic growth. This results in an inverted U-shaped relationship, first proposed to explain the relationship between economic development and inequality.

We fit different polynomial degree equation to capture an traditional EKC and other potential non-linear relationships, we specify a quartic (fourth-degree polynomial) model. Our support sample consists goes from 0.05 to 0.95 of our GDP per capita distribution, excluding extremes that may lead to non-smooth shift to the fitted curves. We use population-weighted regressions to ensure that regions with larger populations have a proportionally greater influence on the estimated coefficients. Our formal specification for the fourth degree polynomial is as follows:

$$AOD_{id} = \alpha + \sum_d \beta_d \ln(GDP_i)^d + \epsilon_i \quad (1)$$

Where i indexes the geographical unit of observation, which varies between different levels of sample aggregation such as Region, Subregion, Country, and Subnational units. d indicates the polynomial degrees, which are from 1 to 4. AOD_i is the population-weighted average Aerosol

Optical Depth, measuring air pollution by aerosol exposure. $\ln(\text{GDP}_i)$ is the natural logarithm of real GDP per capita, our measure of economic development. β_d are the coefficients to be estimated, which jointly determine the shape of the curve. ϵ_i is the stochastic error term, assumed to be independently and identically distributed.

The shape of the curve, and thus the validity of the EKC hypothesis, is determined by the signs and statistical significance of the β_d coefficients. For non-linear polynomials, β_1 indicates how GPD and AOD are related, expected to be positive according to the EKC theory. If an inverted U-shaped curve exists, β_2 is negative, indicating a decreasing relationship between environmental degradation and income. A key estimation performed by the literature on EKC analysis is the identification of turning points, which indicate income levels at which the marginal effect of income on pollution changes sign and the curve starts to fall. We calculate these turning points (TP_d) for non-linear approaches by taking the first derivative of Equation (1) with respect to the log of GDP per capita and setting it to zero. The derivative is as follows:

$$TP_d = \frac{\partial \text{AOD}_{id}}{\partial \ln(\text{GDP}_i)} = 0 \quad (2)$$

The GDP_i that satisfies Equation (2) is the income turning point for a polynomial fit with degree d . We additionally provide confidence interval estimates for this estimate turning point.

3.2 Quantile Regression

The polynomial approach estimates the average relationship between income and air pollution. However, the effect of economic growth may differ significantly across the AOD distribution. To explore this heterogeneity, we employ a conditional quantile regression approach. This method allows us to model the Environmental Kuznets Curve (EKC) not just for the mean, but for various quantiles (τ) of the conditional Air pollution distribution. This reveals whether the income-pollution relationship is different for cleaner (lower quantiles) versus more polluted (higher quantiles) observational units, conditional on their income. We estimate a quadratic model for each quantile $\tau \in \{0.1, 0.2, \dots, 0.9\}$ as follows:

$$Q_\tau(\text{Pollution}_i | \ln(\text{GDP}_i)) = \alpha_\tau + \beta_{1\tau} \ln(\text{GDP}_i) + \beta_{2\tau} \ln(\text{GDP}_i)^2 + \epsilon_{i\tau} \quad (3)$$

Where, Q_τ is the τ -th conditional quantile of pollution for unit i , given its level of GDP per capita. The coefficients α_τ , $\beta_{1\tau}$, and $\beta_{2\tau}$ are specific to each quantile τ and are estimated separately for each quantile.

This approach allows us to address several key questions. First, by comparing the coefficient estimates across different quantiles, we can formally test for differences in the EKC's shape across the pollution distribution. Second, we can calculate quantile-specific turning points (TP_τ) to determine if different percentiles of the air pollution distribution experience their pollution levels peak at different income stages. Using the first derivative condition, we can see that the turning point for a given quantile (TP_τ) is found at the income level where:

$$TP_\tau = \ln(GDP) = -\frac{\beta_{1\tau}}{2\beta_{2\tau}} \quad (4)$$

Similarly to before, the income level which satisfies this condition is the turning point for the conditional quantile group. We use the estimated parameters to derive income elasticities for each subnational unit by associating it with its closest estimated quantile curve and using predicted level of AOD and coefficients to measure the following elasticity equation:

$$\eta_i = \frac{\partial AOD_i}{\partial GDP_i} \times \frac{GDP_i}{AOD_i} = (\beta_{1\tau} + 2\beta_{2\tau}) \times \frac{GDP_i}{\hat{AOD}_i} \quad (5)$$

This provides understanding of how economic growth impacts pollution levels for different parts of the distribution and under varying initial environmental conditions.

4 Results

4.1 Polynomial fit results

Our polynomial analysis reveals a robust cubic pattern for the Environmental Kuznets Curve (EKC) on a global scale and can be seen in Figure 1a. This finding is stable across various group samples and non-linear specifications, not changing the U-inverted pattern. The cubic relationship between income and pollution holds consistently whether using regional, subregional, country, or subnational units. Table 3 shows the estimated coefficients for polynomial specifications using subnational observations. The linear relationship in column 1 is negative, suggesting that income increase reduces air pollution exposure. However, when assuming non-linear functional forms, this coefficient is positive. The second key information is the sign

of the squared log GDP, which is negative in the second column. This reveals that the global curve that relates GDP and air pollution has the inverted U-shape as predicted by the EKC theory. The fitting performance does not change with higher degrees, as R^2 is similar across specifications.

Table 2 shows how the quadratic polynomial fits across different location aggregation samples. The results show that as we increase the number of observations with finer location categories, from the regional to the subnational level, the estimated EKC becomes flatter. This can be seen in the decrease of the coefficient magnitude from -0.53 using continents to -0.12 using subnational units. This suggests that while the overall shape persists, the magnitude of the income effect is lower as we account for within-location group variations. The use of finer datasets, as the subnational data, is important to capture significant within-location variation, allowing to capture more precise estimates.

Table 2 also presents our estimated turning points, where the marginal effect of income on pollution begins to decline, ranging from an income level of \$ 6,727 using continents to \$4,948 per capita when using subnational units. The confidence intervals are more precise when increasing granularity, but the estimate intervals are consistent across samples. We find that the cubic specification is sufficient to capture the data variation. Adding higher-order polynomial terms does not significantly improve the model's fit, indicating that the cubic model provides an adequate and parsimonious representation of the global relationship

4.2 Heterogeneity in Regional and Country-Level EKCs

Although the pooled global polynomial analysis provides a clear and consistent pattern of an EKC, this finding is not consistent within subregions. Figure 2 visualizes what we obtained for each subregional when using a quadratic fit for subnational units. The expected inverted U-shaped curve is not consistent across regions. We find U-shaped, inverted U-shaped, and linear curves for different regions. The country EKC estimations are available in our appendix results, and show the same inconsistency.

This divergence implies that the global EKC is largely an aggregation phenomenon. It represents an average trend that may not accurately describe the developmental trajectory of any individual subregion or country. The lack of a consistent pattern at the finer levels may indicate that different regions of the world are situated in different parts of the EKC path. This is more evident if we consider the concentration of subunits by subregional income. Units are

clusters on the left of the turning point for observations in poorer subregions, whereas richer subregions tend to have units on the right side of the curve.

4.3 Quantile regression results

Figure 3 and table 3 analyze the relationship between subnational air pollution by aerosol (relative to the global mean) and subnational log GDP per capita using a conditional-quantile quadratic model, providing evidence consistent with the Environmental Kuznets Curve (EKC) hypothesis. The results reveal that the curvature of the EKC is highly heterogeneous across the distribution of air pollution.

The estimated curves consistently show an inverted U-shaped relationship, but their shape varies dramatically from the lowest to the highest air pollution quantiles. This is demonstrated by the coefficient for the Log GDP per capita squared term, which measures the rate of decline post-peak. For the 10th quantile (low pollution regions), this coefficient is a relatively mild -0.036 . In stark contrast, for the 90th quantile (high pollution regions), the coefficient is -0.185 (five times larger in magnitude). This indicates that the inverted U curve is much steeper and more sharply defined for regions with historically higher air pollution levels.

The coefficient for Log GDP per capita (the initial ascent) also shows a strong quantile effect. This coefficient is only 0.613 for the 10th quantile, but rises sharply to 3.252 for the 90th quantile. This result suggests that as low-polluting areas develop, the initial rise in aerosol pollution is relatively slow, while regions that are already highly polluted experience a significantly more rapid escalation in pollution as their economic output increases up to the turning point. This difference highlights that the penalty for initial development is much greater for those areas that are already environmentally burdened. The visual evidence in the figure supports this, as the dashed lines (higher quantiles) exhibit a steeper positive slope than the solid lines (lower quantiles) before the peak.

Despite the significant heterogeneity in the curve's curvature and initial slope, the GDP turning point estimates remain relatively consistent across the distribution. The estimated turning points—the GDP per capita level at which pollution begins to decline—range from a low of $\$3,112$ (20th quantile) to a high of $\$6,646$ (90th quantile). The text's specified range from $\$5,403$ (10th) to $\$6,646$ (90th) also emphasizes this clustering. The narrow range suggests that the economic threshold required to shift from a pollution-intensive development path to a cleaner one is remarkably similar for subnational units, irrespective of their baseline air quality

status.

In summary, the conditional-quantile analysis shows that high-pollution subnational regions are characterized by a more intense relationship with economic growth: they experience a faster rise in pollution, but also a sharper potential decline after the EKC turning point is reached. The stability of the turning point estimates, however, suggests that the underlying mechanism that triggers environmental improvement may be tied to a universal level of economic maturity across diverse subnational contexts.

4.4 Elasticities

To provide a more granular understanding of the income-pollution relationship, we move beyond the overall shape of the curve and calculate the pollution-GDP point elasticity for each observational unit. The elasticity, η_i , measures the percentage change in pollution (AOD) resulting from a one percent change in GDP per capita. This allows us to assess the immediate marginal impact of economic growth.

Our elasticity estimation leverages the results from the quantile regressions, and follows three steps. First, for each subnational unit i , we identify its closest conditional quantile curve based on its observed pollution and GDP levels. Second, we select the corresponding estimated coefficients ($\beta_{1\tau}$ and $\beta_{2\tau}$) from that specific quantile, τ . Finally, using these coefficients, we estimate the point elasticity for each unit.

The point elasticity is formally derived from our quadratic EKC specification following Equation (5). Theoretically, the Air pollution elasticity to income is the product of the marginal effect of GDP on AOD and the ratio of GDP to AOD. Which can be interpreted as the percentage variation in Air pollution at the subnational level induced by 1% increase in income. We estimate the subnational unit elasticities and aggregate these units into subregions to derive statistical moments for each of them.

The distribution of subregional and subnational estimated point elasticities can be seen in Figure 4. The results reveal a pattern consistent with a global Environmental Kuznets Curve. On average, the elasticities exhibit a clear trend with respect to income levels across subregions. Low-income regions are characterized by a positive Pollution-GDP point elasticity ($\eta_i > 0$) In these areas, economic growth is still associated with rising pollution levels, indicating that they are on the upwards sloping side of the EKC. In contrast, high-income regions show a negative Pollution-GDP point elasticity ($\eta_i < 0$). For these units, increases in GDP per capita

are associated with reductions in pollution, placing them on the downwards sloping side of the EKC.

Despite this clear global trend, the results highlight considerable heterogeneity within sub-regional groups. At any given level of regional average GDP per capita, there is dispersion of elasticities, underscoring that the relationship between economic growth and environmental quality is not uniform within these location groups.

5 Conclusion

In this paper, we investigate the existence of a global Environmental Kuznets Curve (EKC) using regional, subregional, national, and subnational information on air pollution by aerosol, population estimates, and GDP per capita. We add to the literature by presenting the first global population weight investigation of the EKC curve at the subnational level. The first paper to use an Aerosol Optical Depth as a measure of air pollution by aerosol to investigate the global relationship between income and air pollution by aerosol at the subnational level. We also add to the EKC literature by providing the first quantile regression analysis of the relationship at the subnational level, and estimate subnational pollution-income elasticities for the all globe.

Our results suggest the existence of a global EKC, an inverted U-shaped correlation between income and pollution. This relationship is consistent across different polynomial degree specifications and geographical categorization of the globe. The subnational results indicate a flatter curve, but the same EKC pattern exists.

Quantile regressions show that this world pattern is considerably different for quantiles of the pollution by aerosol distribution. EKC curves for lower quantiles are flatter than the global estimate EKC, and higher quantiles have steeper curves.

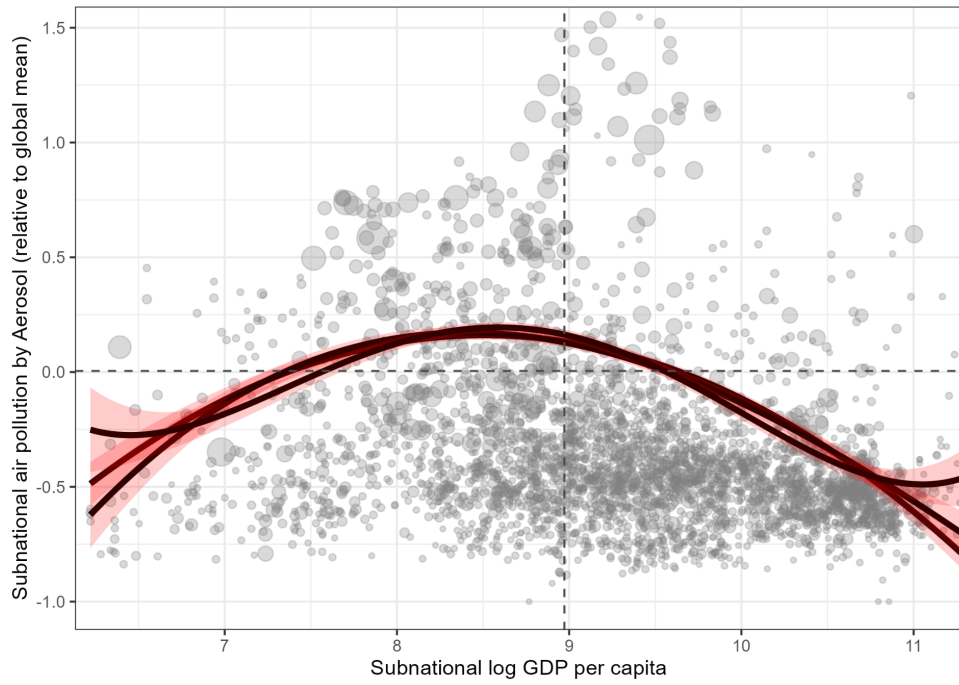
The estimated elasticities add to the evidence of an EKC relationship around the globe. This is indicated by the decrease in Subregional average Pollution-GDP elasticities with income. Poorer regions do have positive elasticities, which turn positive in richer regions. However, there is heterogeneity within regions.

References

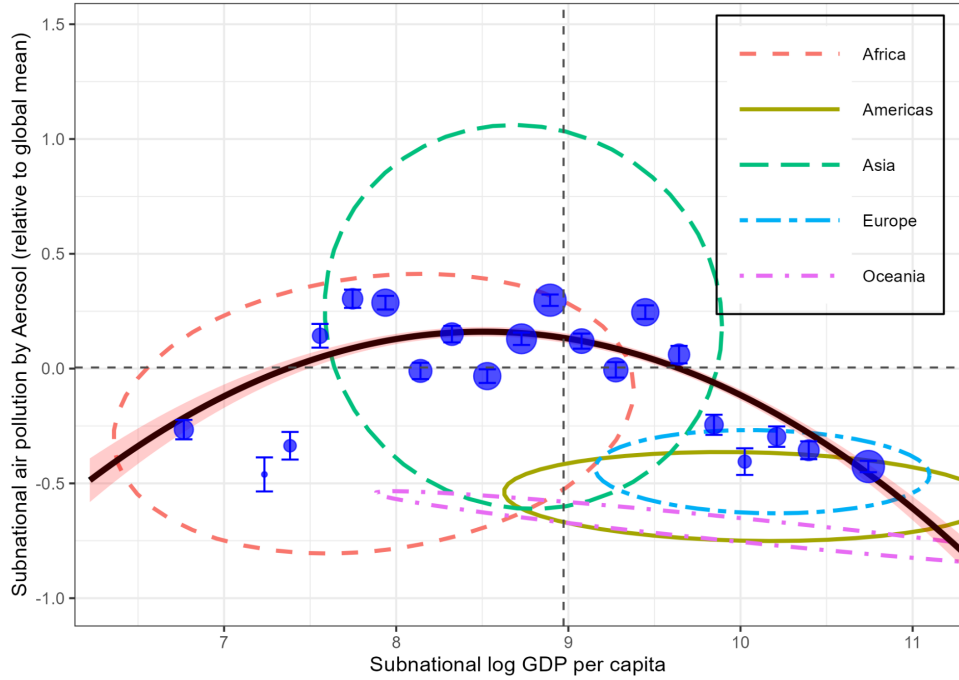
- CIESIN Columbia University. 2018. *Gridded Population of the World, Version 4 (GPWv4): Basic Demographic Characteristics, Revision 11*. Palisades, New York. <https://doi.org/10.7927/H46M34XX>.
- Cohen, Gail, Joao Tovar Jelles, Prakash Loungani, Ricardo Marto, and Gewei Wang. 2019. "Decoupling of Emissions and GDP: Evidence from Aggregate and Provincial Chinese Data." *Energy Economics, Energy Finance* 2017, 77 (January): 105–118. <https://doi.org/10.1016/j.eneco.2018.03.030>.
- Cornillon, P., J. Gallagher, and T. Sgouros. 2003. "OPeNDAP: Accessing Data in a Distributed, Heterogeneous Environment." *Data Science Journal* 2:164–174. <https://doi.org/10.2481/dsj.2.164>.
- Gennaioli, Nicola, Rafael La Porta, Florencio Lopez-de-Silanes, and Andrei Shleifer. 2013. "Human Capital and Regional Development." *The Quarterly Journal of Economics* 128, no. 1 (February): 105–164. <https://doi.org/10.1093/qje/qjs050>.
- Grossman, Gene M., and Alan B. Krueger. 1991. *Environmental Impacts of a North American Free Trade Agreement*. SSRN Scholarly Paper. Rochester, NY, November. <https://papers.ssrn.com/abstract=232073>.
- Hao, Hongfei, Kaicun Wang, Chuanfeng Zhao, Guocan Wu, and Jing Li. 2024. "Visibility-Derived Aerosol Optical Depth Over Global Land from 1959 to 2021." *Earth System Science Data* 16, no. 7 (July): 3233–3260. <https://doi.org/10.5194/essd-16-3233-2024>.
- Hu, Zhiyong. 2009. "Spatial Analysis of MODIS Aerosol Optical Depth, PM2.5, and Chronic Coronary Heart Disease." *International Journal of Health Geographics* 8, no. 1 (May): 27. <https://doi.org/10.1186/1476-072X-8-27>.
- Jacobsen, Jette Bredahl, and Nick Hanley. 2009. "Are There Income Effects on Global Willingness to Pay for Biodiversity Conservation?" *Environmental and Resource Economics* 43, no. 2 (June): 137–160. <https://doi.org/10.1007/s10640-008-9226-8>.
- Jayachandran, Seema. 2022. "How Economic Development Influences the Environment."
- Kummu, Matti, Maija Taka, and Joseph H. A. Guillaume. 2018. "Gridded Global Datasets for Gross Domestic Product and Human Development Index Over 1990–2015." *Scientific Data* 5, no. 1 (February): 180004. <https://doi.org/10.1038/sdata.2018.4>.
- Lenoble, Jacqueline, Lorraine Remer, and Didier Tanre. 2013. *Aerosol Remote Sensing*. Springer Science & Business Media, February.
- Mohsin, Muhammad, Sobia Naseem, Muddassar Sarfraz, and Tamoor Azam. 2022. "Assessing the Effects of Fuel Energy Consumption, Foreign Direct Investment and GDP on CO₂ Emission: New Data Science Evidence from Europe & Central Asia." *Fuel* 314 (April): 123098. <https://doi.org/10.1016/j.fuel.2021.123098>.
- NASA Earth Observatory. 2024. *Aerosol Optical Depth*. https://earthobservatory.nasa.gov/global-maps/MODAL2_M_AER_OD.
- Roy Chowdhury, Rinku, and Emilio F. Moran. 2012. "Turning the Curve: A Critical Review of Kuznets Approaches." *Applied Geography, Environmental Kuznets Curves and Environment-Development Research*, 32, no. 1 (January): 3–11. <https://doi.org/10.1016/j.apgeog.2010.07.004>.
- Stern, David I., and Jeremy van Dijk. 2017. "Economic Growth and Global Particulate Pollution Concentrations." *Climatic Change* 142, no. 3 (June): 391–406. <https://doi.org/10.1007/s10584-017-1955-7>.
- Tanasa, Ioana, Marius Cazacu, Dumitru Botan, John D. Atkinson, Viktor Sebestyen, and Brindusa Sluser. 2025. "From Aerosol Optical Depth to Risk Assessment: A Novel Framework for

- Environmental Impact Statistics of Air Quality Using AERONET." *Environments* 12, no. 8 (August): 285. <https://doi.org/10.3390/environments12080285>.
- Wang, Qingxin, Dongsheng Du, Siwei Li, Jie Yang, Hao Lin, and Juan Du. 2021. "Comparison of Different Methods of Determining Land Surface Reflectance for AOD Retrieval." *Atmospheric Pollution Research* 12, no. 8 (August): 101143. <https://doi.org/10.1016/j.apr.2021.101143>.
- Xiong, Xiaoxiong, Emily J. Aldoretta, Amit Angal, Tiejun Chang, Xu Geng, Daniel O. Link, Vincent V. Salomonson, et al. 2020. "Terra MODIS: 20 Years of on-Orbit Calibration and Performance." *Journal of Applied Remote Sensing* 14, no. 3 (August): 037501. <https://doi.org/10.1117/1.JRS.14.037501>.

Figure 1: Global Polynomial fitted curves



(a) Non-linear Polynomial fitted curves



(b) Non-linear Polynomial fitted curves and continental groups

Notes: These panels show the fitted polynomial curves using subnational units log GDP per capita and Air pollution by aerosol burden. Panel A shows the quadratic, cubic, and quartic fitted curves. Panel B shows different regions of the world.

Table 1: Weighted Regression Results: Air Pollution Burden vs Log(GDP) polynomial terms

	Dependent variable: Air Pollution Burden			
	(1)	(2)	(3)	(4)
Log(GDP)	-0.120*** (0.008)	2.105*** (0.115)	4.874*** (1.156)	-49.971*** (8.696)
Log(GDP) ²		-0.124*** (0.006)	-0.440*** (0.131)	9.043*** (1.496)
Log(GDP) ³			0.012** (0.005)	-0.710*** (0.114)
Log(GDP) ⁴				0.020*** (0.003)
Constant	1.086*** (0.077)	-8.794*** (0.512)	-16.785*** (3.358)	100.969*** (18.807)
Observations	3,712	3,712	3,712	3,712
R ²	0.052	0.140	0.141	0.150
Adjusted R ²	0.051	0.139	0.140	0.149
Residual Std. Error	0.009 (df = 3707)	0.008 (df = 3706)	0.008 (df = 3705)	0.008 (df = 3704)
F Statistic	201.590*** (df = 1; 3707)	300.985*** (df = 2; 3706)	202.848*** (df = 3; 3705)	163.878*** (df = 4; 3704)

Note: This table reports the regressions using polynomial terms using the subnational unit sample. Each column corresponds to a different polynomial degree fit estimated. Standard errors are reported in parentheses.

*p < 0.10, **p < 0.05, ***p < 0.01.

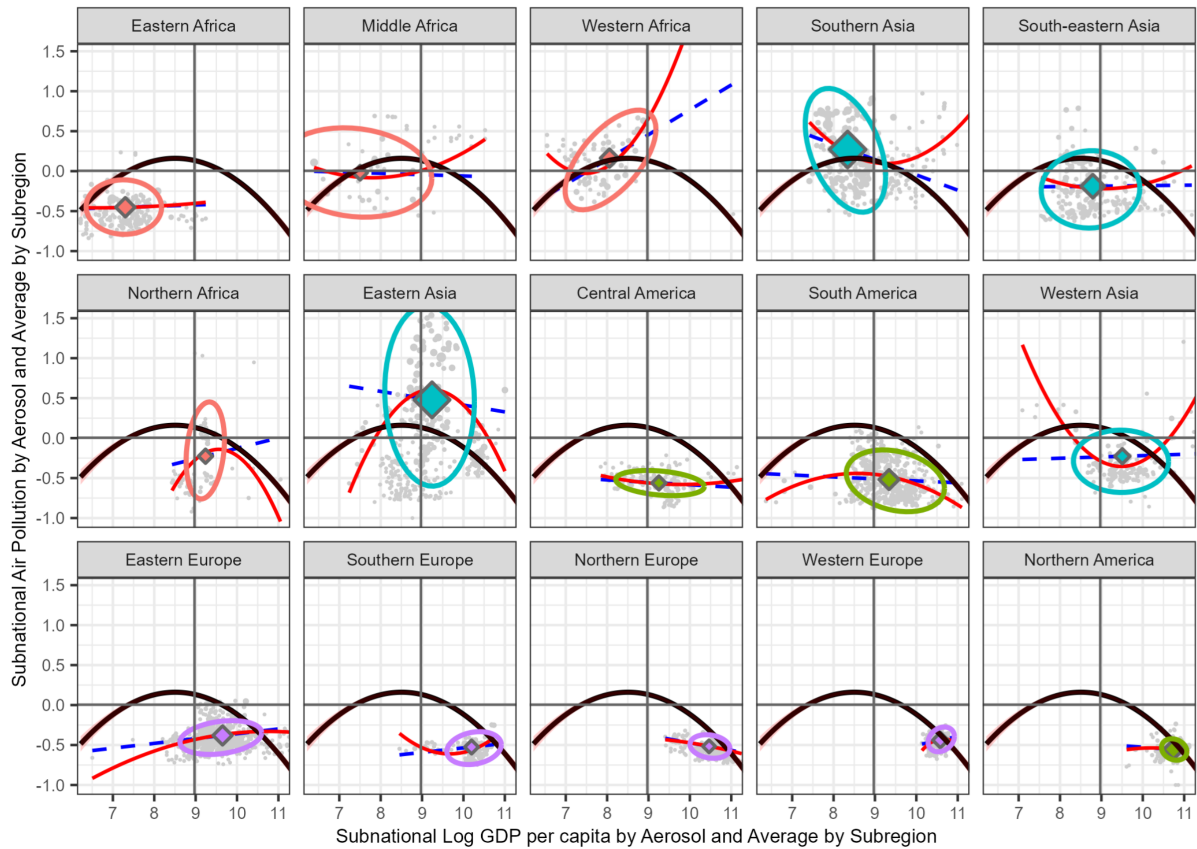
Table 2: Quadratic polynomial regression by different location aggregation groups

	Dependent variable: Population-weighted air pollution by aerosol.			
	Region (1)	Subregion (2)	Country (3)	Subnational (4)
Log(GDP)	9.416* (2.567)	3.537** (1.382)	2.770*** (0.446)	2.105*** (0.115)
Log(GDP) ²	-0.534* (0.141)	-0.204** (0.076)	-0.162*** (0.025)	-0.124*** (0.006)
Constant	-41.253* (11.624)	-15.190** (6.246)	-11.630*** (2.005)	-8.794*** (0.512)
Turning point (GDP per capita, 2010 US Dollars)	6,727	5,897	5,037	4,948
Turning point 95 confidence interval	[5,315 8,513]	[3,563 9,761]	[3,982 6,371]	[4,565 5,363]
Observations	5	22	170	3,712
R ²	0.917	0.351	0.298	0.140
Adjusted R ²	0.833	0.283	0.289	0.139

Note: This table reports the quadratic regression for different aggregation samples. Each column corresponds to a different location aggregation sample. Standard errors are reported in parentheses. The GDP turning point is calculated as $\exp\left(-\frac{\beta_1}{2\beta_2}\right)$, where β_1 and β_2 are the coefficients on log GDP and its square. The 95% confidence intervals for the turning points are reported in brackets.

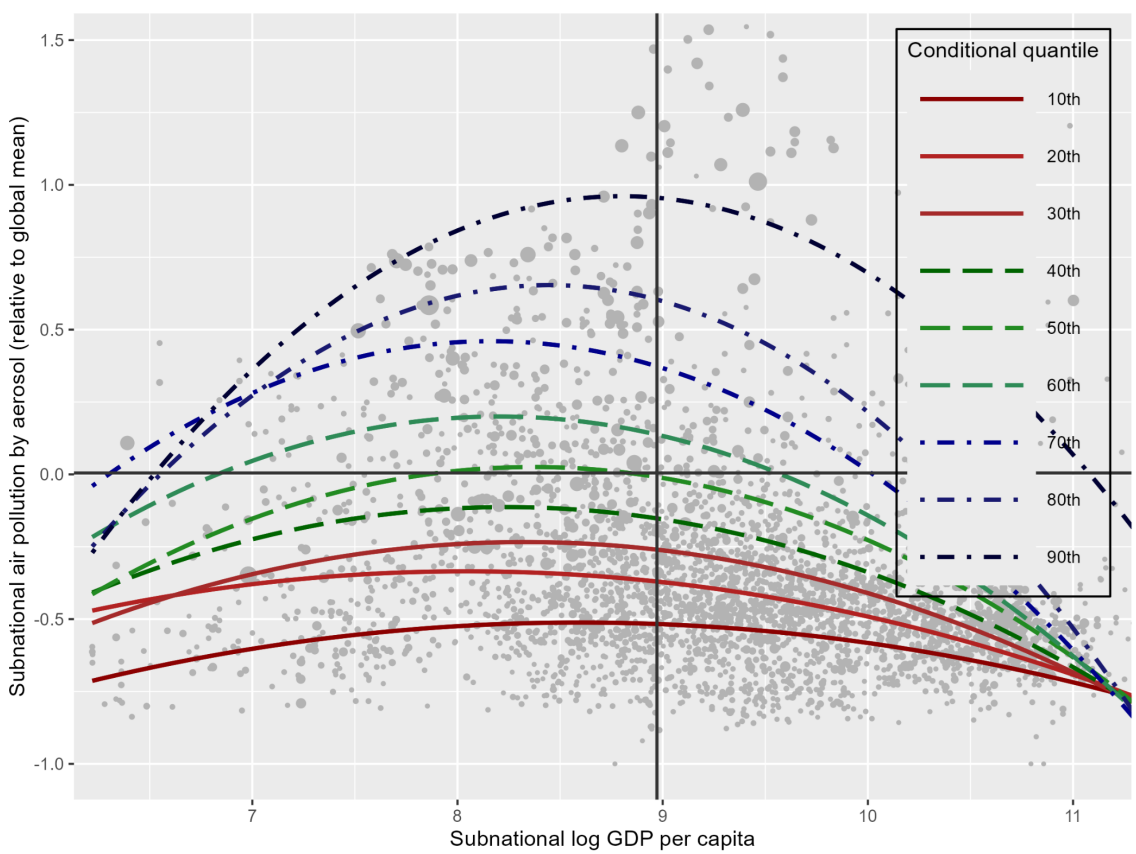
*p < 0.10, **p < 0.05, ***p < 0.01.

Figure 2: Quadratic fitted curves by subregion



Notes: This plot shows the quadratic fitted curves for different subregions of the world. The fitted curve was estimated using 80 percent of the subnational units in the subregions. Subregions are ordered from the lowest to the richest region. X-axis shows subnational Log GDP per capita, and the Y-axis shows Air Pollution burden. Subregions are ordered from the poorest (upper left) to the richest (bottom right).

Figure 3: Quantile estimated curves



Notes: This plot shows the quantile fitted curves. On the x-axis, subnational unit GDP per capita is plotted, and on the y-axis, we plot the subnational air pollution by aerosol burden relative to the global mean. A vertical line is drawn to mark the mean log GDP per capita across subnational units. A horizontal line divides positive and negative air pollution by aerosol burden.

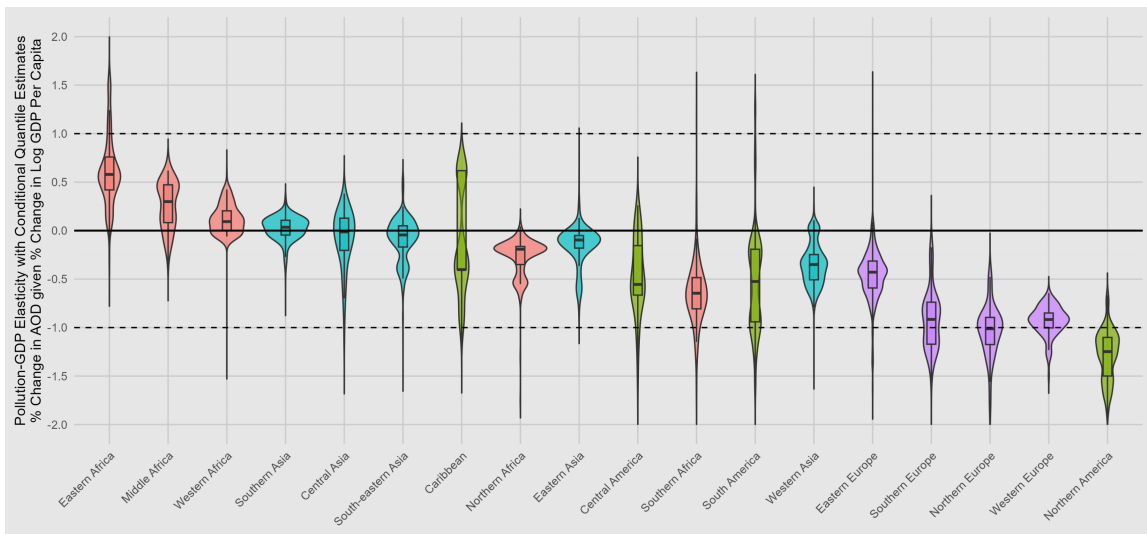
Table 3: Global conditional-quadratic association between population-weighted air pollution by aerosol and GDP per capita (PPP, 2010 US Dollars) at subnational aggregations.

	Dependent variable: air pollution by aerosol								
	10th (1)	20th (2)	30th (3)	40th (4)	50th (5)	60th (6)	70th (7)	80th (8)	90th (9)
Log(GDP)	0.613* (0.326)	0.656* (0.390)	1.049*** (0.166)	1.194*** (0.337)	1.590*** (0.440)	1.736** (0.596)	2.164*** (0.286)	3.074*** (0.490)	3.252*** (0.902)
Log(GDP) ²	-0.036** (0.017)	-0.041* (0.020)	-0.063*** (0.009)	-0.072*** (0.018)	-0.095*** (0.023)	-0.106*** (0.031)	-0.133*** (0.016)	-0.182*** (0.027)	-0.185*** (0.054)
Constant	-3.148** (1.526)	-2.975 (1.845)	-4.602*** (0.738)	-5.033*** (1.587)	-6.630*** (2.073)	-6.920** (2.852)	-8.371*** (1.250)	-12.329*** (2.175)	-13.352*** (3.743)
GDP turning point	5,403	3,112	4,136	3,783	4,316	3,654	3,508	4,664	6,646
Turning point 95 CI	[2,228 13,103]	[667 14,517]	[3,172 5,391]	[1,987 7,204]	[2,400 7,763]	[1,539 8,672]	[2,738 4,494]	[3,781 5,754]	[4,282 10,315]
Pseudo R2	-0.002	-0.108	0.012	0.093	0.085	0.131	0.123	0.169	0.027
Observations	3,712	3,712	3,712	3,712	3,712	3,712	3,712	3,712	3,712

Note: This table reports weighted quantile regression results of air pollution burden on log GDP and its squared term, estimated at the 10th to 90th percentiles of the conditional distribution. Each column corresponds to a different quantile of the outcome variable. Standard errors are reported in parentheses. The GDP turning point is calculated as $\exp\left(-\frac{\beta_1}{2\beta_2}\right)$, where β_1 and β_2 are the coefficients on log GDP and its square. The 95% confidence intervals for the turning points are reported in brackets. Pseudo-R² values correspond to each quantile regression.

*p < 0.10, **p < 0.05, ***p < 0.01.

Figure 4: Estimated subnational GDP-Pollution elasticities by subregion



Notes: The figure plots subnational elasticities by subregions ordered from the poorest to the richest region. Colors sign different continents around the globe. Subregional moments are plotted in a boxplot style, presenting mean, 75th, and 25th percentiles.

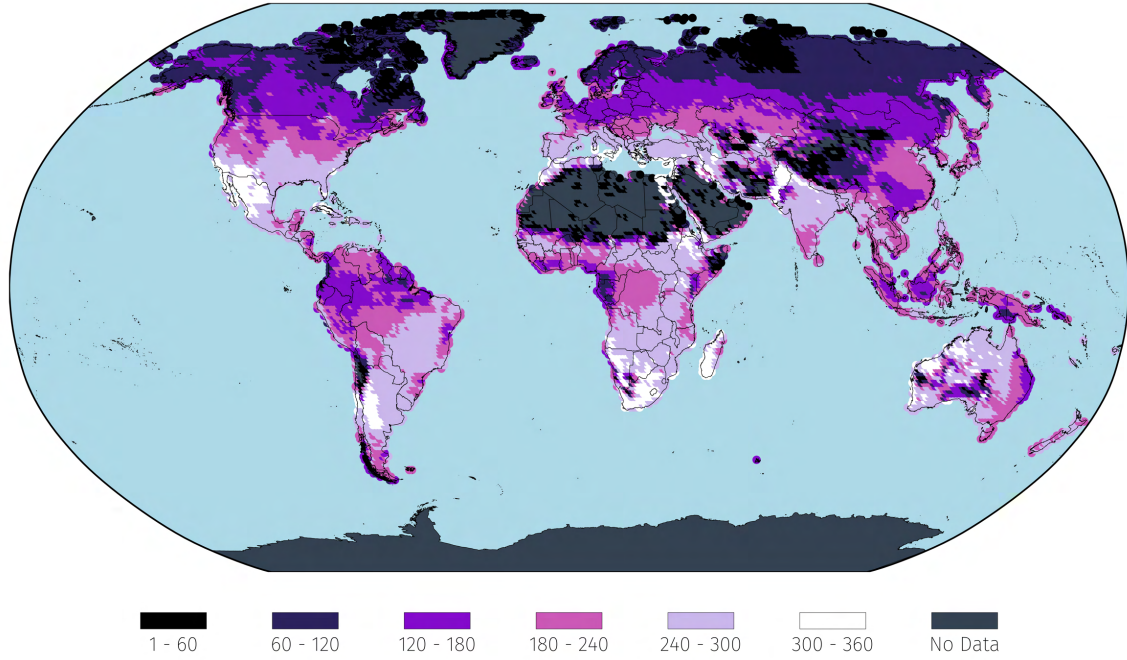
ONLINE APPENDIX

Unfolding the Greener Path: A Global Subnational Analysis of the Environmental Kuznets Curve

Angelo dos Santos, Oscar Morales, Jere R. Behrman, Emily Hannum, Fan Wang

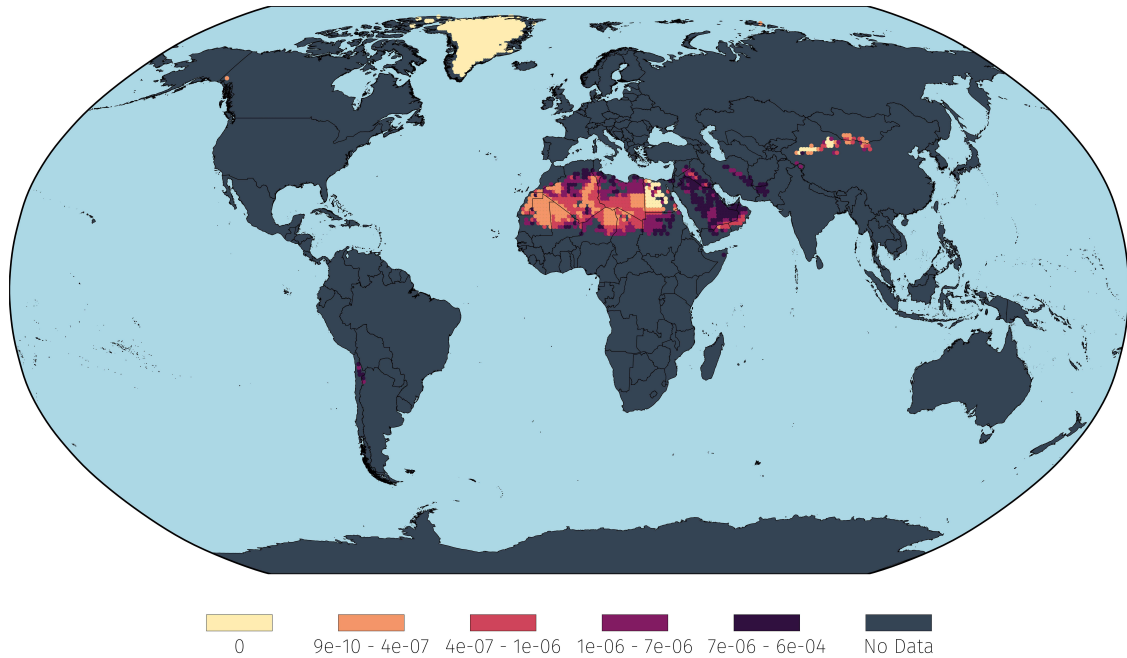
A Additional Figures and Tables

Figure E.1: Number of days with AOD data available for each $1^\circ \times 1^\circ$ longitude–latitude grid, 2010



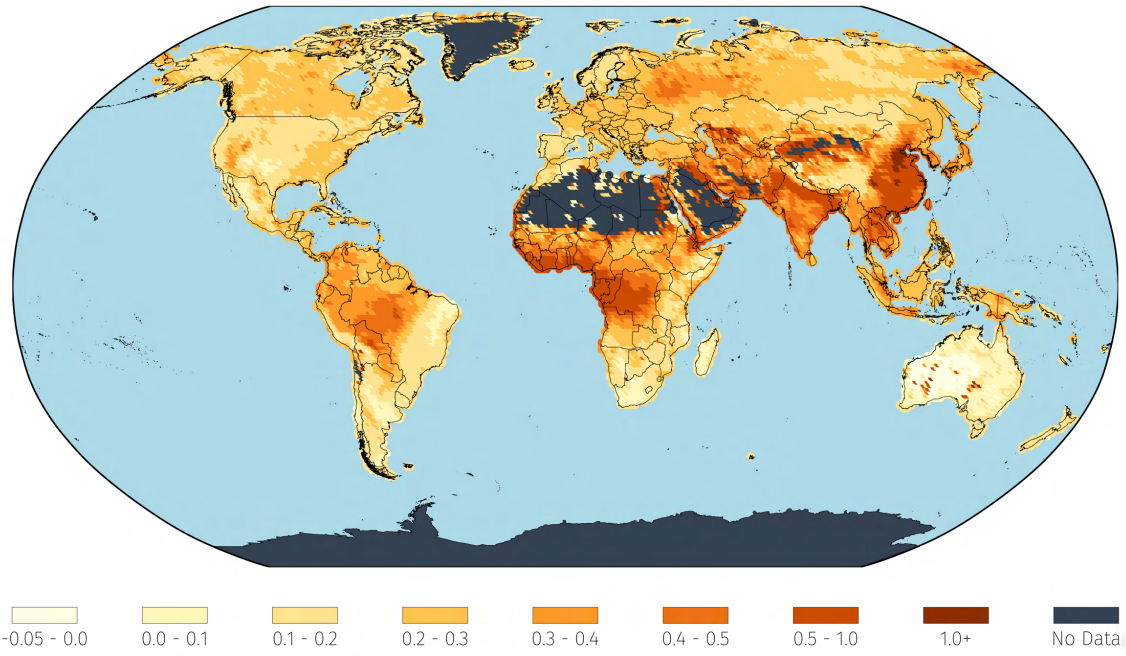
Notes: The figure presents the geographical and temporal availability of Aerosol Optical Depth (AOD) data, our global proxy for ambient particulate matter pollution exposures. For our analysis, we download raw AOD data available at $3\text{km} \times 3\text{km}$ resolution and compute average daily AOD on each day of the year with available AOD measurements for each $1^\circ \times 1^\circ$ longitude–latitude grid (cell). The figure shows the number of days in 2010 during which AOD data was available within each cell. The days are represented through shades of purple and pink from the darkest purple (1 day) to the lightest pink (almost all days in the year); days with zero data are represented by a gray color. Due to the concentration of missing AOD data in regions with the least population, our population-weighted AOD distributional results based on the raw data and interpolated and extrapolated data are very similar. Our global inequality results presented in the text are based on annual averages of the raw data.

Figure E.2: Population shares in areas with no raw AOD measurements $1^\circ \times 1^\circ$ longitude–latitude grid, 2010



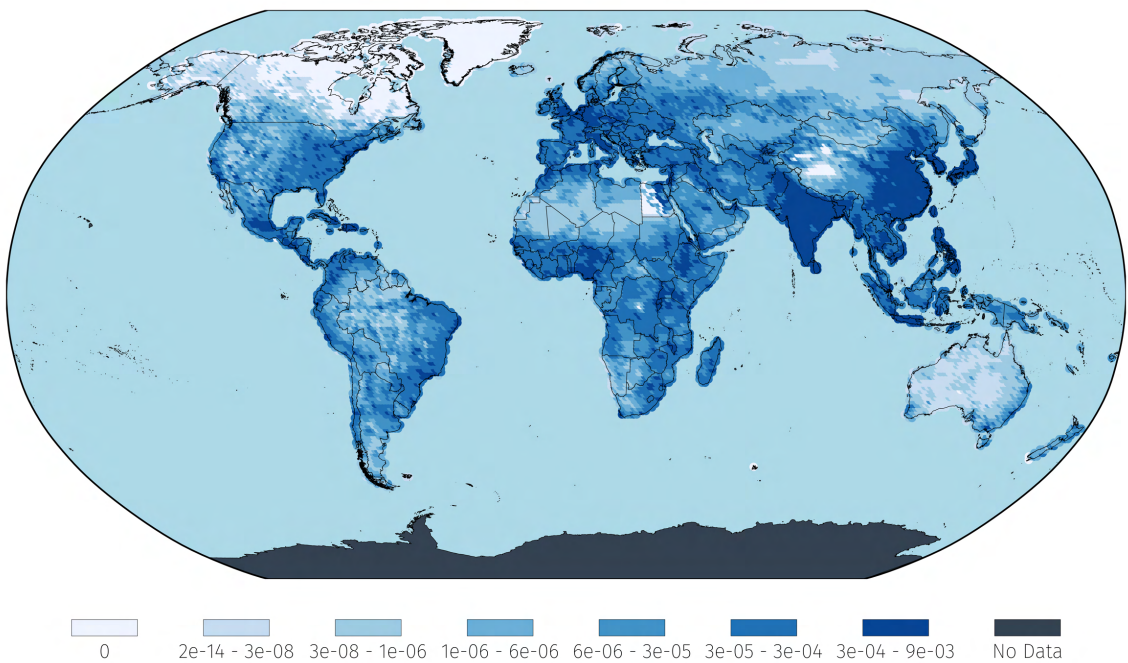
Notes: The figure plots the population shares of areas for which no AOD measurements exist. The share of global population represented by all colored areas amounts to just 0.00602 with 99.8% of cells in this section having a population share below the mean population share (0.000128) in areas with existing AOD measurements. Similarly, 85.8% of cells in this area have values below the median population measure (0.0000069) in areas for which AOD values exist. This means that above-global-average AOD measurements would have to had existed in these areas for our global population-weighted AOD mean to remain the same, otherwise our global mean would be lower than what was calculated meaning relative burden measures can be considered conservative estimates.

Figure E.3: Daily-averaged-then-annualized AOD values for each $1^\circ \times 1^\circ$ longitude–latitude grid, 2010



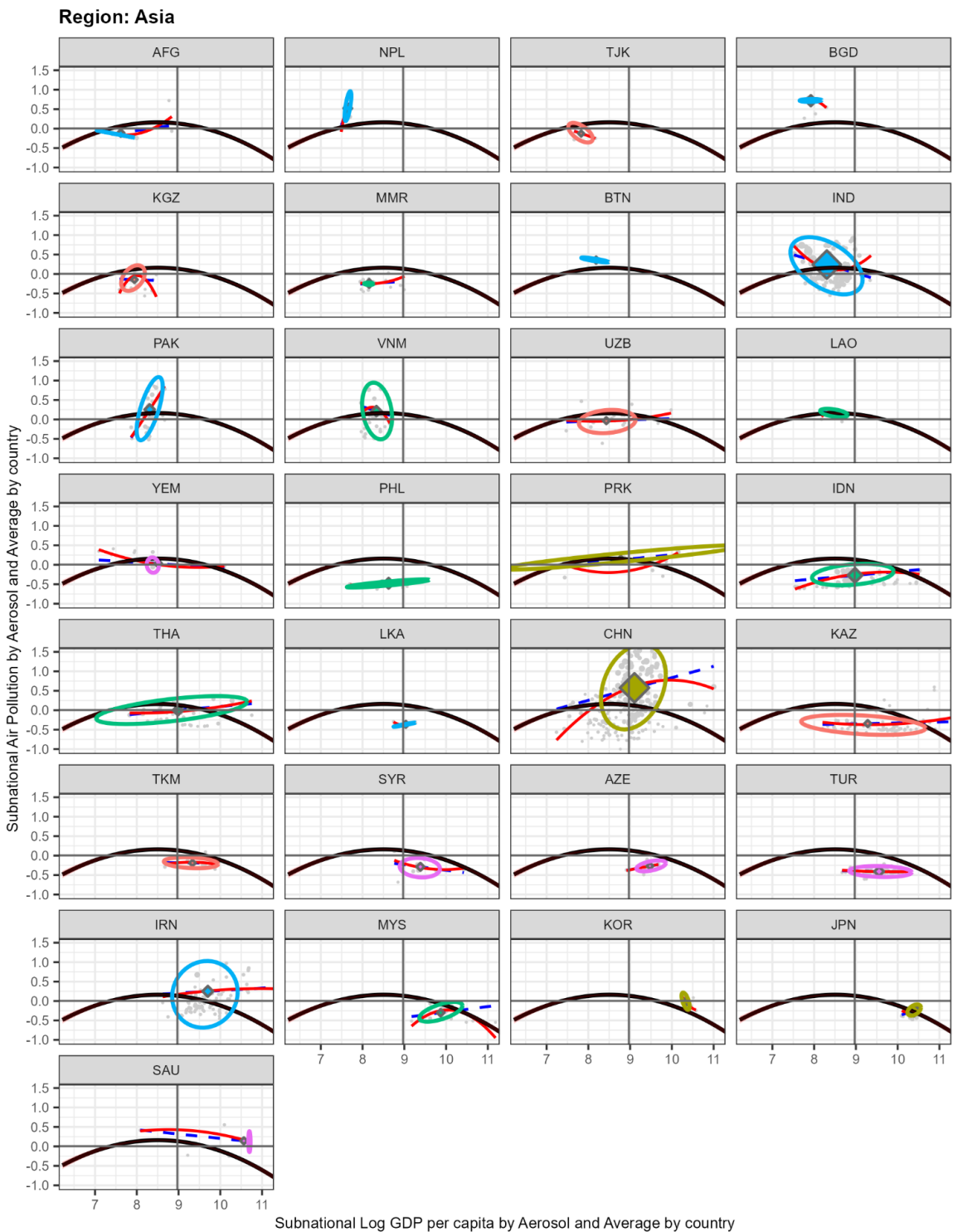
Notes: The figure presents the Aerosol Optical Depth (AOD) values for each coordinate grid, globally, as computed by first averaging collected values in a given day for a given coordinate, for each day, then annualized across daily data, for 2010. Darker shades of orange indicate higher levels of AOD

Figure E.4: GPWv4 population shares for each $1^\circ \times 1^\circ$ longitude–latitude grid, 2010



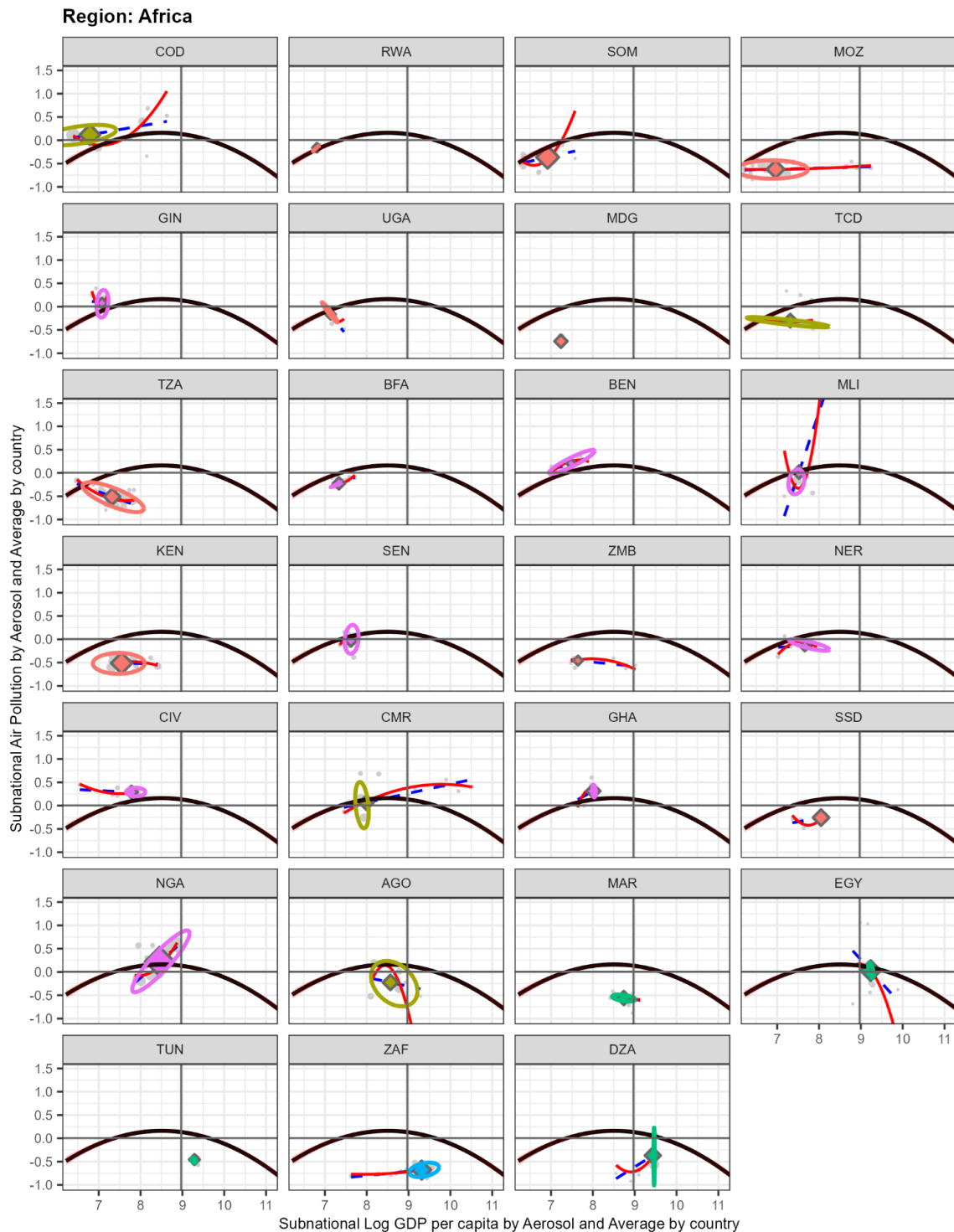
Notes: The figure presents raw population figures as part of SEDAC's GPWv4 population data collection, for 2010. The units of measurements are cell-level global population shares for every $1^\circ \times 1^\circ$ grid. Darker shades of blue indicate a higher population share.

Figure E.5: Quadratic fitted curves for Asian countries



Notes: This plot shows the quadratic fitted curves for different asian countries. The fitted curve was estimated using 80 percent of the subnational units in each country. Subregions are ordered from the lowest to the richest region. X-axis shows subnational Log GDP per capita, and the Y-axis shows Air Pollution burden. Countries are ordered from the poorest (upper left) to the richest (bottom right).

Figure E.6: Quadratic fitted curves for African countries



Notes: This plot shows the quadratic fitted curves for different african countries. The fitted curve was estimated using 80 percent of the subnational units in each country. Subregions are ordered from the lowest to the richest region. X-axis shows subnational Log GDP per capita, and the Y-axis shows Air Pollution burden. Countries are ordered from the poorest (upper left) to the richest (bottom right).